Hydrol. Earth Syst. Sci. Discuss., https://doi.org/10.5194/hess-2018-438
Manuscript under review for journal Hydrol. Earth Syst. Sci.
Discussion started: 5 September 2018

Hydrology and Earth System Sciences
Open Access
Discussions

Flood forecasting in large karst river basin by coupling PERSIANN CCS QPEs with a physically based distributed hydrological model

Ji Li[1]*, Daoxian Yuan[1,2], Jiao Liu[3], Yongjun Jiang[1], Yangbo Chen[4], Kuo Lin Hsu[5], Soroosh Sorooshian[5]

1. School of Geographical Sciences of Southwest University, Chongqing Key Laboratory of Karst Environment, Chongqing, 400715,China
2. Karst Dynamic Laboratory , Ministry of Land and Resources , Guilin 541004 , China
3. Chongqing Hydrology and Water Resources Bureau, Chongqing, 401120 ,China
4. Department of Water Resources and Environment, Sun Yat-sen University, Guangzhou 510275, China
5. Center for Hydrometeorology and Remote Sensing, Department of Civil and Environmental Engineering, University of California, Irvine Irvine, California

*Correspondence: Ji Li (445776649@qq.com)

Hydrol. Earth Syst. Sci. Discuss., https://doi.org/10.5194/hess-2018-438
Manuscript under review for journal Hydrol. Earth Syst. Sci.
Discussion started: 5 September 2018

Hydrology and Earth System Sciences
Discussions

Abstract.

There is no long-term meteorological or hydrological data in karst river basins to a large extent. Especially lack of typical rainfall data is a great challenge to build a hydrological model. Quantitative precipitation estimates (QPEs) based on the weather satellites could offer a good attempt to obtain the rainfall data in karst area. What's more, coupling QPEs with a distributed hydrological model has the potential to improve the precision for flood forecasting in large karst watershed. Precipitation estimation from remotely sensed information using artificial neural networks-cloud classification system (PERSIANN-CCS) as a technology of QPEs based on satellites has been achieved a wide research results in the world. However, only few studies on PERSIANN-CCS QPEs are in large karst basins and the accuracy is always poor in practical application. In this study, the PERSIANN-CCS QPEs is employed to estimate the hourly precipitation in such a large river basin-Liujiang karst river basin with an area of 58,270 km^2. The result shows that, compared with the observed precipitation by rain gauge, the distribution of precipitation by PERSIANN-CCS QPEs has a great similarity. But the quantity values of precipitation by PERSIANN-CCS QPEs are smaller. A post-processed method is proposed to revise the PERSIANN-CCS QPEs products. The result shows that coupling the post-processed PERSIANN-CCS QPEs with a distributed hydrological model-Liuxihe model has a better performance than the result with the initial PERSIANN-CCS QPEs in karst flood simulation. What's more, the coupling model's performance improves largely with parameter re-optimized with the post-processed PERSIANN-CCS QPEs. The average values of the six evaluation indices including Nash–Sutcliffe coefficient has a 14% increase, the correlation coefficient has a 14% increase, process relative error has a 8% decrease, peak flow relative error has a 18% decrease, the water balance coefficient has a 7% increase, and peak flow time error has 25 hours decrease, respectively. Among them, the peak flow relative error and peak flow time error have the biggest improvement, which are the greatest concerned factors in flood forecasting.The rational flood simulation results by the coupling model provide a great practical application prospect for flood forecasting in large karst river basins.

Key words: Quantitative precipitation estimates /QPEs, Precipitation Estimation from Remotely Sensed Information Using Artificial Neural Networks-Cloud Classification System/ PERSIANN-CCS, Liujiang karst river basin , Liuxihe model, Flood forecasting

1 Introduction

The highly anisotropic karst water-bearing media and intricate hydraulic conditions make the karst flood process exhibit significant differences in time and space, which led to the laminar flow and turbulent flow transmute into each other in karst areas, and the flood events in karst river basins are more complicated compared with that of in non-karst area(Ford and Williams,2007;Goldscheider and Drew,2007）.This makes it difficult to precisely simulate and forecast the karst flood process based on a hydrological model in mechanism. It is a common practice that the karst water-bearing media should be simplified before build a model. For example, making karst river basin as a multiple and nested spatial structure; making the underground river as the intelligible river system in the model; cave as the anisotropic medium with a large vertical infiltration coefficient and porosity but small specific yield. Even so, it is still hard to quantify the spatial structure of the karst water-bearing media with a physics-mathematics model. And the karst flood simulation results usually have some errors that could not be ignored, which is the main problem in flood forecasting in karst river basins（Kovacs and Perrochet,2011）.

Because the dynamic change of karst hydrological process and the hydraulic conditions of underlying surface are complicated and non-linear in karst area, which makes it hard to obtain the hydrogeology parameters, such as specific yield, hydraulic conductivity and aquifer transmissivity and so on. With the rapid development of remote sensing, GIS technology and hydrogeology, the technology of field work including the tracer tests (Birk et al.,2005;Doummar et al.,2012) and infiltration tests have made a significant progress. However, it is still a challenge to accurately simulate the laws of motion of the karst hydrological process in the karst water-bearing media with these experimental tests. So the traditional methods such as lumped hydrological models are not suitable for flood forecasting in karst area（Hartmann et al.,2013）. Compared with the performance of lumped hydrological models, the physically based distributed hydrological models (PBDHMs) have some advantages for karst flood forecasting in mechanism. The PBDHMs divide the whole karst river basin into a series of small grid units named karst sub-streams, which could reflect the real rules of hydrological process and karst development characteristics precisely. Therefore, it has a great application potential to improve the karst floods simulation and forecasting capability (Ambroise et al., 1996). Many PBDHMs have been proposed since the blueprint of the PBDHMs published by Freeze and Harlan (1969). The first full PBDHM is regarded as the SHE model published in 1987(Abbott et al., 1986a, b). Shustert and White (1971) used the PBDHM as an attempt in karst area, in their research, the dissolved carbonate species were analyzed in the waters of 14 carbonate springs in the Central Appalachians. And these springs were classified into diffuse-flow feeder-system types and conduit feeder-system types. The PBDHMs have been achieved many good research results in karst area (Atkinson,1977; Quinlan and Ewers,1985;Quinlan et al.,2011;Duan and Miller,1997; Ren,2006;Liu et al.,2013;Zhang et al.,2007).

Since the regulation and storage capacity of the karst water-bearing media are weak. When the accumulated rainfall exceeds the maximum drainage capacity of the channel during a heavy rain storm, then the karst immersion-waterlogging hazard is much more likely to appear in this situation. And the hazard will become more and more serious with the intensification of global extreme weather events. So some effective measures need to be taken

Hydrol. Earth Syst. Sci. Discuss., https://doi.org/10.5194/hess-2018-438
Manuscript under review for journal Hydrol. Earth Syst. Sci.
Discussion started: 5 September 2018

Hydrology and Earth System Sciences
Open Access
Discussions

to reduce the flood losses. For example, simulating and forecasting the karst flood process reliably with a PBDHM effectively, it is an important non-project measure for flood control. However, there is no enough rain gauges as well as the long-term meteorological or hydrogeological data to build a PBDHM in karst river basin where belongs to ungauged basin. Prediction in ungauged basins (PUB) is the theme of international hydrological decade, the core of which is runoff calculation (Li and Ren, 2009). Therefore, it is more difficult to forecast the flood events in karst river basin compared with that of in non-karst area. How to solve the problem of rainfall source is a key factor of the current karst flood forecasting. The quantitative precipitation estimates /QPEs, especially the satellite QPEs technology brings the possibility to obtain the reasonable rainfall data in karst area. But the current application of the QPEs is not mature enough, which makes the accuracy of QPEs as well as the effect of karst flood simulation and forecasting are not so good.

The developed numerical weather prediction model in the past decades provided a reasonable and accurate QPEs product in karst area. The current mainstream QPEs including the weather radar QPEs (Delrieu et al.,2014; Rafieei et al.,2014; Faure et al.,2015), satellite QPEs and radar merging satellite QPEs (Stenz, 2014; Bartsotas et al.,2017; Goudenhoofdt and Delobbe,2009; Wardhana et al.,2017), Precipitation estimation from remotely sensed information using Artificial Neural Networks/PERSIANN QPEs (Soroosh et al.,2000; Hirpa et al.,2010; Romilly, 2011;Yang et al.,2007), PERSIANN-Climate Data Record/PERSIANN-CDR (Ashouri et al., 2014; Liu et al., 2017; Tan and Santo,2018; Hussain et al., 2018), and PERSIANN-Cloud Classification System/PERSIANN-CCS (Yang et al., 2004,2007; Moradkhani and Meskele, 2010）. The research on the QPEs products by meteorological satellites has become a hotspot in rainfall prediction (Hu et al., 2013).

Although many scholars at home and abroad have done a lot of research with the QPEs technology, also achieved many accepted results. However, there are considerable uncertainty exists in the application, which makes the precision of the QPEs is low and the precipitation result by the QPEs is not satisfactory. Two effective measures could reduce the uncertainty of the QPEs results in karst area. One is to match the appropriate resolution of the model. Because the resolution can affect the result of the QPEs directly: if the resolution is too low, then the grid units divided are coarse, which causes a considerable error in rainfall estimates; if the resolution is too high, the meteorological model structure is complicated and unstable. Furthermore, the requirement of computation resources will increase exponentially with the raise of the model spatial resolution (Chen et al., 2017), which leads to huge calculation and low efficiency. So the appropriate model spatial resolution is extremely important for the results of QPEs. And the other is the current technology of QPEs still has some systematic errors existed due to the uncertainties in structure and mathematical algorithm. For this reason, the results of QPEs compared with the observed precipitation by rain gauge have some relative errors, which causes the karst flood simulation results by the coupling model (coupling QPEs with a PBDHM) have uncertainties that affect the model's performance largely. So the results of initial QPEs could not be used directly to build the coupling model. In this study, a post-processed method is employed to revise the PERSIANN-CCS QPEs products, which makes the result of QPEs more credible and receivable.

There are many researches on PERSIANN-CCS QPEs (Yang et al 2007) at present. But most of them have been used in small non-karst watersheds. In this study, the PERSIANN-CCS QPEs is employed to estimate the rainfall data as an attempt in such a large karst river basin -Liujiang Karst River Basin (LKRB) with an area of $5.8*10^4km^2$ in Guangxi province, China. Watershed flood forecasting relies on a PBDHM for a computation tool, while the precipitation is the model's driving force (Li et al., 2017). It has the potential to improve the accuracy of karst flood forecasting by coupling PERSIANN-CCS QPEs with a PBDHM. And the PBDHM in this paper is Liuxihe model（Chen,2009）.The spatial resolution of Liuxihe model for LKRB is 200m*200m. And the PERSIANN-CCS QPEs products that the spatial resolution is 0.04 °*0.04 °scale and time interval is 30 minutes are employed to estimate the precipitation results for LKRB. The resolution of the PERSIANN-CCS QPEs must be downscaled to the same size as Liuxihe model before building the coupling model. The PERSIANN-CCS QPEs products after post-processed could offer the high-precision precipitation results for LKRB where lack of enough rain gauges. It can largely improve the model performance by coupling the post-processed PERSIANN-CCS QPEs with Liuxihe model. A modified PSO algorithm (Chen et al., 2016) is used to optimize the coupling model parameters in this paper, which could control the uncertainty of the parameter passing.

2 Methodology

2.1 PERSIANN-CCS QPEs

The original PERSIANN system (Hsu et al., 1999) was based on geostationary infrared imagery and later extended to include the use of both infrared and daytime visible imagery, which is an automated system for precipitation estimation from remotely sensed information using artificial neural networks .The system for rainfall estimation under development at The University of Arizona and gets constantly stronger with the improvement of the technology (Soroosh et al.,2000). The fundamental algorithm of PERSIANN system is based on a neural network. And the network parameters could be optimized by an adaptive training characteristic, which makes the precipitation could be estimated from geosynchronous satellite at any time and place.

The Precipitation Estimation from Remotely Sensed Information using Artificial Neural Networks-Cloud Classification System /PERSIANN-CCS(Yang et al., 2004; Hsu et al., 2007) is a patch-based cloud classification and rainfall estimation system from low Earth-orbiting

Hydrol. Earth Syst. Sci. Discuss., https://doi.org/10.5194/hess-2018-438
Manuscript under review for journal Hydrol. Earth Syst. Sci.
Discussion started: 5 September 2018

Hydrology and Earth System Sciences
Open Access
Discussions

and geostationary satellites by using pattern recognition technology and computer imaging technology (Yang et al.,2007). Satellite-based precipitation retrieval algorithms use information ranging from visible (VIS) to infrared (IR) spectral bands of Geostationary Earth Orbiting (GEO) satellites and microwave (MW) spectral bands (Hsu et al., 2007).

The QPEs products of PERSIANN-CCS has been generated precipitation estimates at resolution 0.04 °*0.04 °scale and time interval 30 minutes since 2000. The output of PERSIANN-CCS QPEs has been downscaled at 200m*200m as the same spatial resolution as Liuxihe model in LKRB. The hourly precipitation data of the PERSIANN-CCS QPEs are collected and compared with the precipitation observed by rain gauges.

Rainfall estimation from the PERSIANN-CCS consists as the follow steps (Hsu, 2007): (1) IR cloud image segmentation, (2) Characteristic extraction from IR cloud patches, (3) Patch characteristic classification, (4) Obtain the rainfall estimation results of QPEs products, (5) Evaluate and revise the results of QPEs products.

In this paper, the PERSIANN-CCS QPEs real-time data used in LKRB from the current version of PERSIANN-CCS are available and downloadable online (http://hydis8.eng.uci.edu/CCS/).

2.2 Liuxihe model

Liuxihe model proposed by Yangbo Chen (Chen, 2009)of Sun Yat-Sen University, China is employed as the fully distributed hydrological model in this study, which is a physically based distributed hydrological model（PBDHM）mainly for catchment floods simulating and forecasting(Chen et al., 2011, 2016,2017; Li et al., 2017). Liuxihe model earn its name by first successful application in Liuxihe catchment, Guangdong province, China. There are three layers vertically, including the canopy layer, the soil layer and the underground layer in the model and the whole catchment is divided into a great number of grid cells horizontally by using the DEM, which are treated as a uniform basin, and the elevation, land cover type, soil type, and other model elements including rainfall-runoff, evapotranspiration and so on are calculated on the uniform basin. All cells are categorized into three types, namely hill slope cell, river cell and reservoir cell.

An improved PSO algorithm (Chen et al., 2016) is employed to optimize the model parameters in this study, which can make the model's performance much better in flood forecasting in karst river basins. The observed meteorological, hydrological data and the development conditions of the karst underground river are used to optimize the model parameters. The terrain property data like the DEM, land use type and soil type can be downloaded freely from an open access databases on the website. The model is validated by observed karst flood events. All these factors of the model are physically based and rational to truly reflect the underlying surface of the karst basin. So it implied Liuxihe model could be used for real-time flood forecasting in karst river basins.

Hydrol. Earth Syst. Sci. Discuss., https://doi.org/10.5194/hess-2018-438
Manuscript under review for journal Hydrol. Earth Syst. Sci.
Discussion started: 5 September 2018

Hydrology and Earth System Sciences
Open Access
Discussions

2.3The improvement of the Karst hydrological model

Liuxihe model has been applied successfully for floods forecasting in many river basins. However, all these basins are non-karst areas. This is the first time the model is used in karst river basin as an attempt in this study. And the structure of the model should be improved to suit the karst basins. So some effective measures should be taken before building the model. Firstly, simplify the karst water-bearing media, including making karst basin as a multiple and nested spatial structure, underground river as the intelligible channel system in the model, cave as the anisotropic medium with a large vertical infiltration coefficient and porosity but small specific yield, and fault as the anisotropic medium with a vertical, large infiltration coefficient and specific yield. Secondly, the whole karst river basin will be divided into many small karst sub-basins by the theory of distributed hydrological model. Furthermore, the karst sub-basins will be divided into many karst hydrology respond units (KHRUs), which are generally independent of each other. The whole karst hydrological process including the storage and regulation process of the epikarst zone, the spatial interpolation of the precipitation, evapotranspiration and rainfall-runoff are all calculated on the KHRU. After that, these hydrological processes will be summarized in the karst sub-basins. Then the outlet flow will be formed through the river confluence among each karst sub-basin from upstream to downstream. Such a multi-structure distributed hydrological model could utilize various scale information effectively and make the best use of the observed meteorological, hydrological and geological data.

The whole karst river basin is composed by many small karst sub-basins, then the karst sub-basins will be divided into many KHRUs. And each KHRU has its own model characteristics such as the meteorological and hydrological characteristics as well as the karst development characteristics in this study. The KHRU is proposed to describe the spatial variation of the karst sub-basins. And make sure that the differences within the KHRUs are smaller than of among the KHRUs. Then the KHRU is divided into five layers vertically: the canopy layer, the soil layer, the epikarst zone, the bedrock and the underground river. The sketch map of the KHRU is as follow:

The structure of the KHRU(Ren,2006)   b. The photograph of the three-dimensional space structure of the KHRU

Figure 1. Sketch map of the KHRU

In Figure 1.b, the three-dimensional space model of the KHRU in Liujiang Karst River Basin(LKRB) is built in the laboratory to better understand how groundwater move in the karst media and convert mutually with the surface river. Then the hydrological model could be built more visualized through this way.

In order to satisfy the applicability of the model in karst area, the epikarst zone as a distinctive structure of the KHRU is considered carefully in the model. An exponential decay equation is used to calculate the regulation and storage process of surface karst zone. The linear reservoir model is employed to describe the regulation process of the superficial karst fissure system. And the Muskingum routing method is used to calculate the convergence process of the karst underground river that will be summarized and converge to drainage outlet through the underground river system.

The karst hydrological process of the epikarst zone could be divided into rapid fissure flow and slow fissure flow. When the precipitation falls to the surface karst zone, it will fill the pores of the macro crack firstly. After all the pores are full-filled, means the macro crack is saturated. This part of saturated water content named rapid fissure flow will go directly into the underground river through the macro crack, and ignore the regulation and storage hydrological process of the macro crack in this study. The rest of the water content will enter the tiny pores in the surface karst zone, and the water content of rapid fissure flow could be described as the following equation:

$$SW_{epi} = Q_{\inf} - V_{crk} \tag{1}$$

Where SW_{epi} is the water content of the rapid fissure flow in the epikarst zone,

$Q_{\inf}$ is the infiltration water content, and V_{crk} is the water content in the macro crack.

The slow fissure flow in the epikarst zone is calculated by an exponential decay equation (Ren, 2006):

$$\begin{cases} W_{sep} = W_{epi}\left(1-\exp\left(\dfrac{-\Delta T}{TT_{\mathrm{perc}}}\right)\right) \\ W_{epi,\ t+1} = W_{epi,t} + SW_{epi,t+1} - W_{sep,t+1} \\ TT_{\mathrm{perc}} = \dfrac{SAT_{epi} - FC_{epi}}{K_{epi}} \end{cases} \tag{2}$$

Where W_{sep} is the water content from the epikarst zone to the underground river, W_{epi} is the current water content of the epikarst zone, ΔT is the simulation time-step, TT_{perc} is the attenuation coefficient, SAT_{epi} is the saturation water content of the epikarst zone, FC_{epi} is field capacity of the epikarst zone, and K_{epi} is the saturated hydraulic conductivity of the epikarst zone.

The linear reservoir model is employed to calculate the regulation process of the superficial karst fissure system, and the base discharge is calculated by the hydraulic gradient of the KHRU (Neitsch et al.,2000) :

$$\begin{cases} Q_{gw} = 8000\dfrac{K_{epi}h_{wtbl}}{\left(L_{gw}\right)^2} \\ Q_{gw,i} = Q_{gw,i-1}\exp\left(-a_{gw}\Delta t\right) + W_{rchrg}\left[1-\exp\left(-a_{gw}\Delta t\right)\right] \\ W_{rchrg,i} = W_{seep}\left[1-\exp\left(-\dfrac{1}{\delta_{gw}}\right)\right] + W_{rchrg,i-1}\exp\left(-\dfrac{1}{\delta_{gw}}\right) \end{cases} \tag{3}$$

Where Q_{gw} is the base discharge, $Q_{gw,i}$ and $Q_{gw,i-1}$ is the supplies quantity of the base discharge that converge to the karst conduit or underground river on the i and (i-1) day respectively, K_{epi} is the saturated hydraulic conductivity of the epikarst zone, h_{wtbl} is the hydraulic gradient, L_{gw} is the length of the KHRU, a_{gw} is the depletion coefficient of the base discharge, ΔT is the simulation time-step(day), $W_{rchrg,i}$ is the supplies quantity of the aquifer on the i day(mm/d), W_{seep} is the water flux through the bottom of the soil profile into the underground aquifer on the i day （mm/d）, δ_{gw} is the delay time of the supplies（day）.

The Muskingum routing method is used to calculate the convergence process of the karst underground river in this study, the equation is as follows:

$$W = K[xI + (1-x)O] = KO' \tag{4}$$

Where O' is the water storage content, O is the outlet flow of the river reach, x is the dimensionless proportion factor, I is the inflow discharge of the river reach, K is the slope of the correlation curve of the water storage content and the discharge.

The finite difference method is used to calculate the water balance equation and the Muskingum routing method:

Hydrol. Earth Syst. Sci. Discuss., https://doi.org/10.5194/hess-2018-438
Manuscript under review for journal Hydrol. Earth Syst. Sci.
Discussion started: 5 September 2018

$$\begin{cases} O_2 = C_0 I_2 + C_1 I_1 + C_2 O_1 \\ C_0 + C_1 + C_2 = 1 \end{cases} \tag{5}$$

where,

$$\begin{cases} C_0 = \dfrac{0.5\Delta t - Kx}{0.5\Delta t + K - Kx} \\ C_1 = \dfrac{0.5\Delta t + Kx}{0.5\Delta t + K - Kx} \\ C_2 = \dfrac{-0.5\Delta t + K - Kx}{0.5\Delta t + K - Kx} \end{cases} \tag{6}$$

If the parameter of the Muskingum routing method *K* and *x* could be determined for a karst underground river reach, then the value of the C_0, C_1 and C_2 will be calculated by the equation(6). When $\Delta t = 2Kx$, $C_0 = 0$, which means the karst flood forecasting lead time will be 2*Kx*, then the Muskingum routing method could be simplified as follows:

$$O_2 = C_1 I_1 + C_2 O_1 \tag{7}$$

One of the key problems of Muskingum routing method is to optimize the parameters -*K* and *x* in the practical application. The least square method is used in this study:

$$\min \left\{ E = \sum_{j=1}^{n} \{ W_0(j) - W_1(j) - C]^2 \right\} \tag{8}$$

Where *E* is the objective function between the observed water storage content and the simulated one, which makes only require least squares approximation with regard to functional value, $W_0(j)$ and $W_1(j)$ are the observed and simulated water storage content at j period respectively, $W_1(j) = K[xI + (1-x)O]$, *n* is the total numbers of the observation periods, C is the absolute value of the water storage content.

In order to simplify calculating, making *A=K*x, B=K*(1-x)*, then taking the partials with respect to *A, B, C* respectively:

$$\begin{cases} \sum W_0 I = A\sum I^2 + B\sum(OI) + C\sum I^2 \\ \sum W_0 O = A\sum(OI) + B\sum O^2 + C\sum O \\ \sum W_0 I = A\sum I + B\sum O + Cn \end{cases} \tag{9}$$

Hydrol. Earth Syst. Sci. Discuss., https://doi.org/10.5194/hess-2018-438
Manuscript under review for journal Hydrol. Earth Syst. Sci.
Discussion started: 5 September 2018

Then the values of *A*, *B*, *C* could be calculated as follows:

$$\begin{cases} A = \dfrac{y_1}{y_2} - \dfrac{y_3}{y_2} \\ B = \dfrac{y_1 z_2}{y_3 z_2} - \dfrac{y_2 z_1}{y_2 z_3} \\ C = \sum \dfrac{W_0 - A\sum I - B\sum O}{n} \end{cases} \qquad (10)$$

Where,

$$\begin{cases} y_1 = \sum (W_0 I) - \dfrac{\sum W_0 \sum I}{n} \\ y_2 = \sum I^2 - \dfrac{(\sum I)^2}{n} \\ y_3 = \sum (IO) - \dfrac{\sum O \sum I}{n} \\ z_1 = \sum (W_0 O) - \dfrac{\sum W_0 \sum O}{n} \\ z_2 = \sum O^2 - \dfrac{(\sum O)^2}{n} \\ z_3 = \sum IO - (\dfrac{\sum O \sum I}{n}) \\ K = A + B \\ x = \dfrac{K}{A} \end{cases} \qquad (11)$$

The parameters of the Muskingum routing method could be optimized through the above equations. And after that, the convergence process of the karst underground river could be calculated by the Muskingum routing method in Liuxihe model.

3 Study area and data

3.1 Study area

Liujiang Karst River Basin (LKRB) in southern China is selected as the study area in this paper. It is the second largest tributary of Pearl River that covers three provinces including Guizhou, Guangxi and Hunan province. LKRB is the most developed karst area of China with a drainage area of 58270km^2 and a channel length of 1121 km. The carbonate rocks are widely distributed in the southwest of the basin, and the areas account for 33% of the whole watershed. LKRB is a typical karst-mountainous catchment with frequent flash flooding in the past centuries .The peak forest-plain area is the main karst landform on the ground, while the karst conduit and fissure are well-developed underground, also there are many complicated underground rivers and springs with large flow (Li, 1996). The karst water-bearing media is highly non-linear and heterogeneous, which makes it very difficult to simulate and forecast the karst hydrological process.

LKRB is in the sub-tropical monsoon climate zone with an average annual precipitation of 1400mm to 1700mm, and the precipitation distribution is highly uneven at spatial and temporal scale. The precipitation from April to September accounts for 75% to 80% of the annual precipitation.

After studied the karst geomorphology of LKRB, Wil1iams (1987) believed that the peak-cluster depression had developed into turreted peak-forest landforms after a long evolutionary process, which is equivalent to the late prime of life, and going into the old age of geomorphologic evolution as the tradition physiognomy theory by Davis (1912). The allogenic water especially the Liujiang river is the main driving force for the development of peak-forest landforms. Therefore, the peak-forest plains and valleys are often distributed in contiguous areas near the main trunk stream of the Liujiang river. And the main karst landform of LKRB is peak-forest plain, there are also some peak-cluster depressions and peak-forest valleys. Figure 2. are the DEM and three-dimensional topographical map of LKRB.

a. the DEM b. three-dimensional topographical map

Figure 2. The DEM and three-dimensional topographical map of LKRB.

3.2 Rain gauges and the karst flood process

There are 68 rain gauges and 131 grid points of PERSIANN-CCS QPEs within LKRB and five karst flood events from 2008 to 2013 has been collected respectively. There is a flood event each year. The karst floods process in LKRB have typical characteristics: the flood peak flows usually exceed 10,000m^3/s and expression of the multi-peaks flood process. A flood process usually lasts about 10 days, and the shortest flood event duration is only about 3 days, the longest is 25 days. The hourly precipitation data of rain gauges are collected in this study to compare with the results of PERSIANN-CCS QPEs. The rain gauges, grid points of PERSIANN-CCS QPEs and the Liuzhou river gauge that closes to the outlet of LKRB are shown in Figure 3.

Figure 3. Sketch map of Liujiang River Basin（LKRB）

Hydrol. Earth Syst. Sci. Discuss., https://doi.org/10.5194/hess-2018-438
Manuscript under review for journal Hydrol. Earth Syst. Sci.
Discussion started: 5 September 2018

Hydrology and Earth System Sciences
Open Access
Discussions

3.3 Property data

Catchment property data for distributed hydrological model mainly include DEM, land use and soil types. These data are downloaded from an open access databases. The DEM is downloaded from the shuttle radar topography mission database at http://srtm.csi.cgiar.org (Falorni et al., 2005, Sharma et al., 2014). The downloaded DEM has an initial spatial resolution of 90m*90m, and after many model resolution tests, the most appropriate resolution has been confirmed as 200m*200m for Liuxihe model in LKRB. So the spatial resolution of the initial DEM is rescaled to 200m*200m in this study, which is a high resolution for Liuxihe model in LKRB. The DEM is shown in Figure 2(a).The land use type is downloaded from http: //landcover.usgs.gov (Loveland et al., 1991, 2000), and the soil type is downloaded from http://www.isric.org. The initial spatial resolutions of the land use type and soil type are 1000m*1000m. Both of them need to be rescaled to 200m*200m in this study. Figure 4 (a) is land use types and (b) is soil types.

Figure 4. The property data for Liuxihe model in LKRB

4 PERSIANN-CCS QPEs and its post-processed results

4.1 Precipitation estimation results

The QPEs product of PERSIANN-CCS has been generated precipitation result for LKRB in this study. There are 131 grid points of PERSIANN-CCS QPEs within LKRB , which are representative and can cover the whole watershed completely (as shown in Figure 3).The precipitation estimation results by PERSIANN-CCS QPEs has been downscaled as the same temporal-spatial resolution as Liuxihe model, the spatial resolution is 200m*200m and the time interval is 1 hour. The QPEs products of PERSIANN-CCS in 2008,2009,2011,2012 and 2013 are produced respectively, means there are five rainfall events are corresponding to the five karst flood processes. Figure 5-9 is the average precipitation pattern comparisons of two precipitation products in the five years, and (a) is the average precipitation of rain gauges, (b) is the average precipitation of PERSIANN-CCS QPEs.

Figure 5. Precipitation pattern comparison of two precipitation products(2008), (a) is the average precipitation of rain gauges, (b) is the average precipitation of PERSIANN-CCS QPEs.

Figure 6. Precipitation pattern comparison of two precipitation products(2009), (a) is the average precipitation of rain gauges, (b) is the average precipitation of PERSIANN-CCS QPEs.

Figure 7. Precipitation pattern comparison of two precipitation products(2011), (a) is the average precipitation of rain gauges, (b) is the average precipitation of PERSIANN-CCS QPEs.

Figure 8. Precipitation pattern comparison of two precipitation products(2012), (a) is the average precipitation of rain gauges, (b) is the average precipitation of PERSIANN-CCS QPEs.

Figure 9. Precipitation pattern comparison of two precipitation products(2013), (a) is the average precipitation of rain gauges, (b) is the average precipitation of PERSIANN-CCS QPEs.

According to the results of Figure 5-9, it appears that the temporal average precipitation pattern of both products are quite similar, especially in the rainfall distribution, while there are some difference in the quantitative value. The results of PERSIANN-CCS QPEs are smaller than that of the rain gauge, which means there is a relative error exists between the two products.

4.2 Evaluation of PERSIANN-CCS QPEs

In order to quantitatively evaluate the results of PERSIANN-CCS QPEs, the precipitation by PERSIANN-CCS QPEs and rain gauge are compared in this study. The rainfall distribution of both products are shown in Figs. 5–9.To make further comparison, the average precipitation of the five karst flood events are calculated in Table 1.

Table1. Precipitation pattern comparison of two precipitation products

According to the results of Table 1, it could be found that there are obvious relative errors between the two precipitation products. The average precipitations of PERSIANN-CCS QPEs are smaller than that of the rain gauge. For the five karst flood events from 2008 to 2013, the relative errors between two products are -16%,-25%,-14%,-21% and -23% respectively. The average relative error is -20% and the maximum error is -25%, which means these relative errors could not be ignored. So the precipitation results by PERSIANN QPEs must to be revised effectively, the precipitation data observed by rain gauge are used to revise the results of PERSIANN QPEs in this study.

4.3 The post-processed PERSIANN-CCS QPEs

In order to make the results of PERSIANN QPEs more credible and receivable, the precipitation results by PERSIANN QPEs are revised with the observed precipitation by rain gauge. Firstly, finding the grid points of PERSIANN-CCS QPEs that are adjacent the rain gauges (as shown in Figure 3). And there are 23 grid points in LKRB. Secondly, calculating their average precipitation of PERSIANN-CCS QPEs and rain gauges, and taking the average precipitation of rain gauges as the true precipitation. Thirdly, revising the results of PERSIANN QPEs with the average precipitation observed by rain gauges.The procedure is summarized as follows.

1). Calculating the average precipitation of these 23 grid points based on PERSIANN-CCS QPEs with the following equation.

Hydrol. Earth Syst. Sci. Discuss., https://doi.org/10.5194/hess-2018-438
Manuscript under review for journal Hydrol. Earth Syst. Sci.
Discussion started: 5 September 2018

Hydrology and Earth System Sciences
Open Access
Discussions

$$\bar{P}_{PERSIANN-CCS} = \frac{\sum_{i=1}^{N} P_i F_i}{N} \qquad (1)$$

Where, $\bar{P}_{PERSIANN-CCS}$ is the average precipitation of these 23 grid points by PERSIANN-CCS QPEs; P_i is the precipitation based on PERSIANN-CCS QPEs on the i grid point; F_i is the catchment area of the i grid point; N is the number of the grid points.

2). Calculating the average precipitation of these 23 rain gauges.

$$\bar{P}_2 = \frac{\sum_{j=1}^{M} P_j}{M} \qquad (2)$$

Where, $\bar{P}_2$ is the average precipitation observed by these 23 rain gauges; P_j is the precipitation by the j rain gauge; M is the number of rain gauges.

3). The precipitations observed by the adjacent rain gauges are used to revise the results of PERSIANN-CCS QPEs with the following equation.

$$P_i^{'} = P_i \frac{\bar{P}_2}{\bar{P}_{PERSIANN-CCS}} \qquad (3)$$

Where, $P_i^{'}$ is the value of precipitation based on PERSIANN-CCS QPEs after revised on the i grid point; $\bar{P}_2 / \bar{P}_{PERSIANN-CCS}$ is the revise factor.

4). The precipitation results based on PERSIANN-CCS QPEs after revised will be as input data for Liuxihe model to test its feasibility through the floods simulation.

From the above procedure of the post-processed PERSIANN-CCS QPEs, it could be found that the revise factor- $\bar{P}_2 / \bar{P}_{PERSIANN-CCS}$ is a key to make the results of PERSIANN-CCS QPEs much closer to the observed precipitation by rain gauges, means the systematic errors of the PERSIANN-CCS QPEs could be corrected effectively. So the post-processed

Hydrology and Earth System Sciences Discussions
Open Access

method in this paper is a feasible and necessary. And it could greatly improve the accuracy of the coupling model in karst flood simulation and forecasting. Furthermore, the revise factor could be preserved as an empirical value for the future flood forecasting in LKRB.

5 Model set up

5.1hydrological model setup

The method combining DEM with stream network leads to a more accurate drainage network from surface runoff modelling (Li and Tao,2000), especially in karst area. In this study, according to the high resolution of 200m*200m for Liuxihe model in LKRB, the whole studied area is divided into 1,469,900 grid cells named the karst sub-basins by using the DEM. The grid cells include 1,463,204 hill slope cells and 6,696 river cells. Then the karst sub-basins will be divided into many karst hydrology respond units (KHRUs) further, the KHRU is as shown in Figure 1. The river system are divide into three-order by Strahler method (Strahler,1957) as shown in Figure 3.

Because of the sinkholes and karst depressions in karst watershed, as well as the systematic error of the DEM itself, there are many pits including the true and false pits in LKRB. Among them the true pits are the karst depressions and sinkholes, they usually have a certain scale with elevation difference. While the false pits are just few points with low elevation, which is due to the systematic errors of the DEM. So the true and false pits should be distinguished reliably before using DEM data to divide into the karst sub-basins. Firstly, finding out all the pits with low elevation, and connect them into a plane, then distinguish the true pits from the false ones according to the on-site topographic survey. Finally,keeping the true pits like the sinkholes and karst depressions unchanged but filling the false pits in the model.

The karst hydrology respond unit (KHRU) is introduced in this study to reasonably describe the spatial variability of the karst water-bearing media (as shown in Figure1). The spatial characteristic of every KHRU has definite physical meaning. So the calculation of the evapotranspiration, rainfall-runoff and parameter optimization on the KHRU is also physically based, which could truly reflect the differences of the underlying surface. After the division of the karst sub-basins and the KHRUs, the post-processed PERSIANN-CCS QPEs results will be as the input data for Liuxihe model to simulate and forecast the karst flood process. The performance of the coupling model could be improved reliably in this way.

5.2 Parameter optimization of coupling model

There are many parameters need to be optimized for a distributed hydrological model, as shown in Table.2, among them the parameters of soil water properties, the epikarst zone and the underground river are the most sensitive parameters for the coupling model in this study. The parameters of the epikarst zone are the most complicated due to the anisotropy of the karst water-bearing media, which makes it hard to measure and calculate the hydraulic characteristics. According to the field survey, the epikarst zone is mainly developed on the hard surface of pure carbonate rock, especially on the Paleozoic limestone. The thickness and characteristics of the epikarst zone are different due to the different climate, topography and landforms. And the thickness of the epikarst zone is about 10 meters in the study area- LKRB. The parameters of the coupling model are listed inTable 2.

Table 2. The parameters of the coupling model

The parameters of the Soil type like the saturated water content and field capacity are calculated through a software tool by the research result of Saxton (Saxton et al.,1986) .The statistical relation between the soil texture and the soil water could be queried easily in the software tool. And it has been effectively proved by many experiments (Servat and Sakho,1995), the calculated value of this method has a good fitting relation with the measured value.

Liuxihe Model has been deployed on a supercomputer system with parallel computation technology (Chen et al., 2011) .An improved PSO algorithm (Chen et al., 2017)is employed to optimize the parameters of the coupling model in this study. And the flood process for parameter optimization is the Flood 2009060908. The results of parameters optimization are shown in Figure 10, among them, (a) is the objective function evolution result, (b) is the parameters evolution result, and (c) is the simulated flood process by using the optimized model parameters.

Figure 10. Parameter optimization results with the improved PSO algorithm

From the results of Figure 10(c), it could be found that the coupling model with initial model parameter values does not simulate the observed karst flood process satisfactorily, and compared with that, the parameters optimization with the improved PSO algorithm could largely improve the coupling model's performance. The simulated flood process is very close to the observed value.

In order to test the parameters optimization effect with different precipitation sources, both the precipitation of the rain gauge and PERSIANN CCS QPEs are used to optimize the parameters of the coupling model. To compare with that, the simulated flood process of the

Hydrol. Earth Syst. Sci. Discuss., https://doi.org/10.5194/hess-2018-438
Manuscript under review for journal Hydrol. Earth Syst. Sci.
Discussion started: 5 September 2018

Hydrology and Earth System Sciences Discussions

coupling model with the same parameter as rain gauges and re-optimized parameter with the post-processed PERSIANN CCS QPEs are also drawn in Figure 10(c).

From the results of Figure 10(c), it could be found that the coupling model with the re-optimized parameters by the post-processed PERSIANN CCS QPEs has a better flood simulation effect than that of with the same parameter as rain gauges precipitation, which means re-optimized parameters with the post-processed PERSIANN CCS QPEs for the coupling model is necessary.

5.3 Model validation

The karst flood process for parameter optimization is the Flood 2009060908 in this study. Other four floods including Flood 200806090200, Flood 201106010900, Flood 201206022000 and Flood 201306011400 are used to validate the performance of the coupling model. The flood simulation results are drawn in Figure 11.

Figure 11. The flood simulation results of the coupling model with two precipitation products

From the result of Figure 11, it could be seen that the simulated karst flood discharges with the precipitation of rain gauge are the best. And the simulated values are the closest to the measured values, especially the simulated flood peaks are satisfactory, which is the most concerned factor in real-time flood forecasting. The average values of six evaluation indices, including the Nash–Sutcliffe coefficient (C), correlation coefficient (R), process relative error (P), peak flow relative error (E) ,water balance coefficient (W), and peak flow time error (T) are 0.86, 0.86, 18%, 4% , 0.91, and -7 hours respectively (as shown in Table 3). This means parameters optimization with the improved PSO algorithm in this study is effective. From Figure 11, it may be seen that the karst flood simulation results with the initial PERSIANN CCS QPEs are not so satisfactory, and the performance of the model are worse than that of the rain gauge precipitation. While the flood simulation results of the coupling model with the post-processed PERSIANN CCS QPEs are much better, also the evaluation indices of the flood simulation have been largely improved.

6 Results and discussions

In order to test the effects of the flood simulation of the coupling model with the post-processed PERSIANN-CCS QPEs as well as the coupling model with different parameters. Two test methods are used in this paper:

1) Keeping the coupling model parameters unchanged, means the coupling model takes the same parameters as the precipitation of the rain gauge. The flood simulation effects with the initial PERSIANN-CCS QPEs and the post-processed ones could be compared in this way.

2) Re-optimizing the coupling model parameters, means the post-processed PERSIANN-CCS QPEs are used to re-optimize the coupling model parameters again to test its necessity.

6.1 Results of flood simulation with the post-processed PERSIANN-CCS QPEs

After the correction, the post-processed PERSIANN-CCS QPEs precipitation has become much closer to the observed precipitation of rain gauge. In order to analyze the effects of flood simulation with the post-processed PERSIANN-CCS QPEs, five karst flood events including Flood 200806090200, 200906090800, 201106010900, 201206022000 and 201306011400 are used in this paper, and the flood simulation results with different precipitation sources including the rain gauges precipitation, the PERSIANN-CCS QPEs and its post-processed results are compared in Figure 11. In this simulation, keeping the coupling model parameters unchanged, means the coupling model with the same parameters as the rain gauges precipitation, not the re-optimized parameters with the post-processed PERSIANN-CCS QPEs results. The flood simulation results are shown in Figure 11.

From Figure 11, it could be seen that the simulated flood discharges with the precipitation of rain gauge are better than that of the PERSIANN-CCS QPEs. And the simulated peak flows with the PERSIANN-CCS QPEs are lower than the observed ones. However, the flood simulation effects with the post-processed PERSIANN-CCS QPEs make a great progress, the simulated flood processes fit the observation values reasonably, and simulated peak flows are much closer to the observation ones. It implies that the flood forecasting capability has been largely improved by the post-processed method of the PERSIANN-CCS QPEs.

To further compare the flood simulation results, six evaluation indices are calculated and listed in Table 3. It has been found that all the six evaluation indices of rain gauges are better than that of PERSIANN-CCS QPEs. And the indices of QPEs have been improved a lot with the post processed QPEs. The average value of Nash–Sutcliffe coefficient has a 7% increase, the correlation coefficient has a 8% increase, process relative error has a 6% decrease, peak flow relative error has a 14% decrease, the water balance coefficient has a 5% increase, and peak flow time error has 7 hours decrease, respectively. Among them, the peak flow relative error has the biggest improvement. It is obvious that the evaluation indices are improved substantially with the post-processed QPEs. So it implies the post-processed method for PERSIANN-CCS QPEs in this paper is feasible and effective. And coupling the post-processed PERSIANN-CCS QPEs with Liuxihe model has the potential to improve the model performance in flood simulation and forecasting in LKRB.

Hydrol. Earth Syst. Sci. Discuss., https://doi.org/10.5194/hess-2018-438
Manuscript under review for journal Hydrol. Earth Syst. Sci.
Discussion started: 5 September 2018

Hydrology and Earth System Sciences
Open Access
Discussions

6.2 Effects comparison of different model parameters

The performance of the coupling model makes a big difference with different parameters. There are two different sets of model parameter values in this study, one is the parameters with the precipitation of rain gauge, and the other is the parameters with the post-processed PERSIANN-CCS QPEs. The post-processed PERSIANN-CCS QPEs are used to re-optimize the coupling model parameters again to test its necessity. And the flood simulation results with two different sets of model parameters are shown in Figure 12.

Figure 12. Coupled flood simulation results with the same parameter as the rain gauge precipitation and re-optimized parameter with the post-processed PERSIANN-CCS QPEs

From the above results in Figure 12, it has been found that the simulated flood results with re-optimized parameters by the post-processed PERSIANN-CCS QPEs are much better than that of with the same parameter as rain gauge precipitation. The simulated flood discharge processes, especially the peak flows with the re-optimized parameter are closer to the observation values. To further compare the flood simulation results, six evaluation indices are calculated in Table 4, the average value of Nash–Sutcliffe coefficient has a 7% increase, the correlation coefficient has a 6% increase, process relative error has a 2% decrease, peak flow relative error has a 4% decrease, the water balance coefficient has a 2% increase, and peak flow time error has 18 hours decrease, respectively. What is more, comparing with the simulated flood results of the initial PERSIANN-CCS QPEs in Table 3, the average value of Nash–Sutcliffe coefficient has a 14% increase, the correlation coefficient has a 14% increase, process relative error has a 8% decrease, peak flow relative error has a 18% decrease, the water balance coefficient has a 7% increase, and peak flow time error has 25 hours decrease, respectively (as shown in Table 3 and Table 4). So it implies the re-optimized parameters with the post-processed PERSIANN-CCS QPEs for the coupling model is necessary and effective, which makes a better performance for the coupling model in karst flood simulation and forecasting.

6.3 Peak flow time error analysis

It is very important to accurately determine the flood peak flow time in karst area, which could offer enough response times for evacuation safely and rapidly before the flood disaster appears. From the above results in Figure 11, 12 and Table 3, 4, it has been found that all flood simulations have significant peak flow time errors, and all of them are negative, means the simulated flood peaks appeared earlier than the observed values. Among them the average peak flow time error with the precipitation of rain gauge is -7 hours, and that is -32 hours with the precipitation of the initial PERSIANN-CCS QPEs. It is an obvious error and could not be ignored in flood forecasting. While the average peak flow time error of the coupling model with the post-processed PERSIANN-CCS QPEs precipitation and re-optimized parameters is also -7 hours. It makes a great difference. It has been found that both the average peak flow time errors of Liuxihe model with the precipitation of rain gauge and the coupling model with the precipitation of the post-processed PERSIANN-CCS QPEs and re-optimized parameters are -7 hours (as shown in Table 4). So it implies the peak flow time error is -7 hours for the coupling model in LKRB, means the actual time of the flood peak may be 7 hours later, which is very important in flood forecasting and equivalent to a 7 hours long lead time for evacuation safely.

There are two reasons for the peak flow time errors. One is the systematic error of the coupling model itself. And that could be reduced by improving the model structure and function as well as the reliable precipitation by PERSIANN-CCS QPEs and parameters optimization. The other is due to the karst development laws and the characteristics of karst water-bearing media, which can regulate the rainfall process during floods. The karst depressions and other karst negative landforms in the upstream regions can hold back and store some large floods. What is more, the karst fissures can also slow down the floods rate. These factors can play a crucial role in natural flood detention and peak clipping. So the response times of flood peak flow to rainfall increased, and the observed flood peak times lagged behind. In comparison, the simulated flood peak flows appear ahead of time.

The rainfall process from the sky to the ground and finally converge to the outlet of the basin has passed through the surface karst zone, the karst conduit and fissure as well as the underground river. And the karst development laws and the characteristics of karst water-bearing media have obvious influence on the rainfall-runoff process during the whole hydrological process, which makes the response time of flood peak flow to rainfall increases, and the simulated flood peak flow by the coupling model appears earlier. It implies there is a lead time for evacuation safely in flood forecasting.

The flood peak flow time has a very close relationship with the floods rate, and the floods rate is very important to determine the key factors of the karst conduit, the underground river and other hydrogeological parameters. The sensitive parameters in this paper such as the underground river parameters (as shown in Table 2) could be estimate from the floods rate to build the coupling model in karst areas. According to the survey data and tracing test in the study area – LKRB, the flow rate of floods is about 8.64-17.28km/d in dry season; that is 17.28-43.2 km/d in the normal season and is 43.2-129.6 km/d in flood period. The extreme flow rate can reach 172.8km/d, means the karst conduit is very developed in LKRB.

7 Conclusion

There is no reliable precipitation data of rain gauges in many karst river basins. How to obtain the reasonable rainfall data for the hydrological model in flood forecasting is especially

Hydrol. Earth Syst. Sci. Discuss., https://doi.org/10.5194/hess-2018-438
Manuscript under review for journal Hydrol. Earth Syst. Sci.
Discussion started: 5 September 2018

important. In this study, the PERSIANN-CCS QPEs could offer effective precipitation results for the study area. And after the correction, the post-processed PERSIANN-CCS QPEs coupled with a distributed hydrological model-Liuxihe model is proposed in karst flood simulation and forecasting in LKRB. The purpose is not only to simulate the flood process well, but also to find out the key factor how the karst hydrological process responds to the rainfall process in the coupling model. The coupling model employed in this paper has a good performance in flood events simulation, which can offer a reasonable theoretical guidance for flood forecasting, control and disaster reduction in karst river basins like LKRB. Based on the study results, the following conclusions could be drawn:

1). The quantitative precipitation estimates produced by the PERSIANN-CCS QPEs are quite similar to the observed precipitation by rain gauges, especially in the rainfall distribution. But the PERSIANN-CCS QPEs underestimates the precipitation value. The average precipitation is 0.29 for rain gauges and 0.23 for PERSIANN-CCS QPEs.

2). The average relative error is 20% between the two precipitation products. And this relative error could be reduced reasonably by the post-processed method in this paper. The average values of the six evaluation indices including the Nash–Sutcliffe coefficient (C), correlation coefficient (R), process relative error (P), peak flow relative error (E), water balance coefficient (W), and peak flow time error (T) with the initial PERSIANN-CCS QPEs are 0.66,0.69,0.28, 24%, 0.81 and -32 hours, respectively, while those with the post-processed QPEs are 0.73, 0.77, 0.22, 10%,0.86 and -25 hours, respectively. It means the method used in this study for QPEs post-processed is effective, and could improve the effect of the PERSIANN-CCS QPEs capability.

3). The coupling model parameters should be re-optimized using the post-processed PERSIANN-CCS QPEs. Because it has a better performance in the flood simulation than the same model parameters as rain gauges. The average value of Nash–Sutcliffe coefficient (C), correlation coefficient (R), process relative error (P), peak flow relative error (E) ,water balance coefficient (W), and peak flow time error (T) with the same model parameters as rain gauge are 0.73, 0.77, 0.22, 10%,0.86 and -25 hours, respectively, but those with the re-optimized model parameters are 0.80, 0.83, 0.20, 6%,0.88 and -7 hours, respectively. It improves the model performance significantly.

4). The simulated karst floods process based on the precipitation observed by rain gauges is the best. And the flood simulation results by PERSIANN-CCS QPEs after post-processed and re-optimized model parameters could make the coupling model performance much better. The average value of Nash–Sutcliffe coefficient has a 14% increase, the correlation coefficient has a 14% increase, process relative error has a 8% decrease, peak flow relative error has a 18% decrease, the water balance coefficient has a 7% increase, and peak flow time error has 25 hours decrease, respectively. Among them, the peak flow relative error and peak flow time error have the biggest improvement, which are the greatest concerned factors in a flood forecasting in karst river basins.

Data availability

The rain gauge precipitation and river flow discharge data are provided by the Bureau of Hydrology, Pearl River Water Resources Commission, China, exclusively used for this study. The PERSIANN QPEs data are provided by Center for Hydrometeorology and Remote Sensing, Department of Civil and Environmental Engineering, University of California, Irvine. The Liuxihe model used in this study is provided by Yangbo Chen, Department of Water Resources and Environment, Sun Yat-sen University, Guangzhou , China

Competing interests.

The authors declare that they have no conflict of interest.

Acknowledgements. This Study is supported by the Open Project Program of Chongqing Key Laboratory of Karst Environment (Grant No. Cqk201801). The Chongqing Municipal Science and Technology Commission Fellowship Fund (No. cstc2016jcyjys0003), and the National key research and development program of China (2016YFC0502306)

Edited by: Ji Li

Hydrol. Earth Syst. Sci. Discuss., https://doi.org/10.5194/hess-2018-438
Manuscript under review for journal Hydrol. Earth Syst. Sci.
Discussion started: 5 September 2018

Hydrology and Earth System Sciences
Open Access
Discussions

Figures

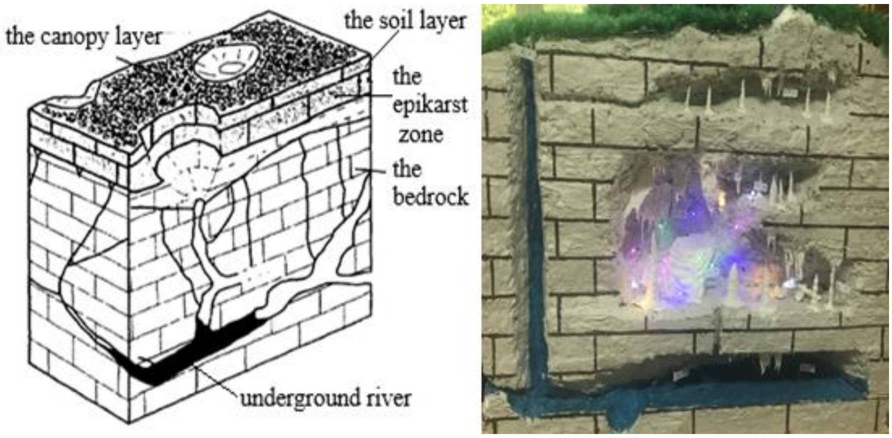

a. The structure of the KHRU(Ren, Q.W.,2006) b. The photograph of the three-dimensional space structure of the KHRU

Figure 1. Sketch map of the KHRU

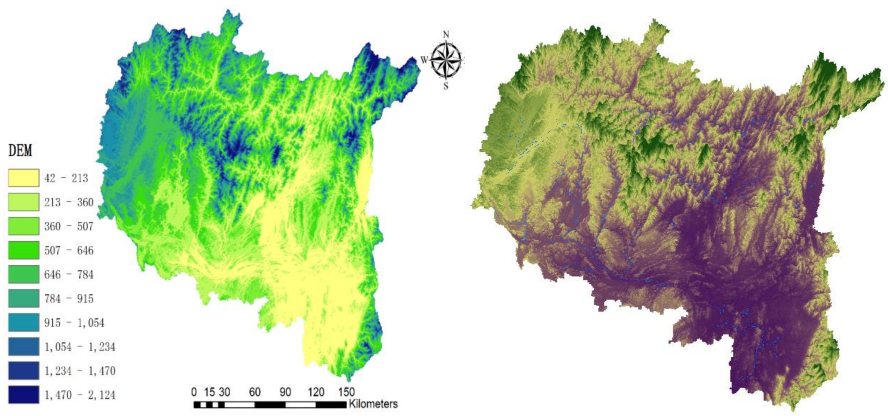

a. The DEM map b. Three-dimensional topographical map

Figure 2. The DEM and three-dimensional topographical map of LKRB.

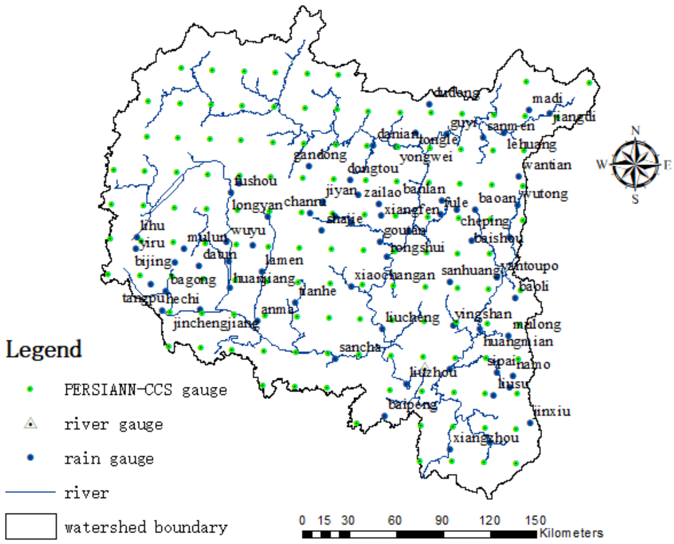

Figure 3. Sketch map of Liujiang River Basin（LKRB）

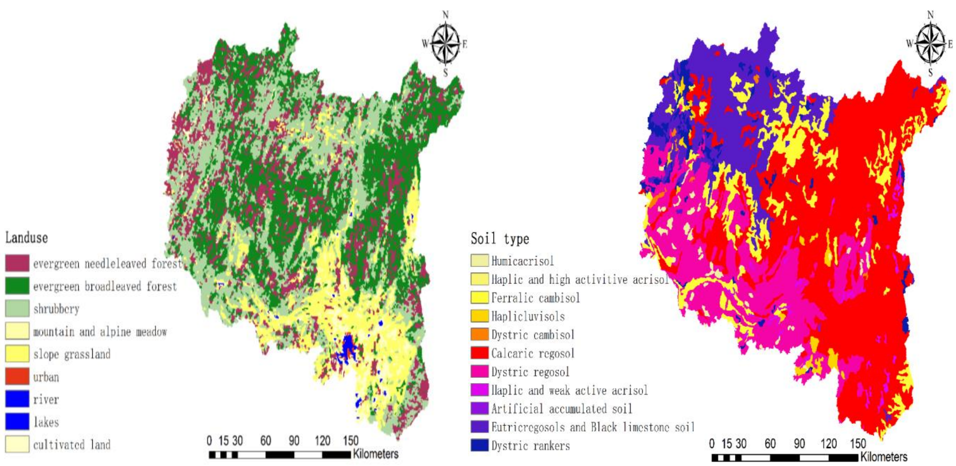

(a) Land use (b) Soil type

Figure 4. The property data for Liuxihe model in LKRB

Hydrol. Earth Syst. Sci. Discuss., https://doi.org/10.5194/hess-2018-438
Manuscript under review for journal Hydrol. Earth Syst. Sci.
Discussion started: 5 September 2018

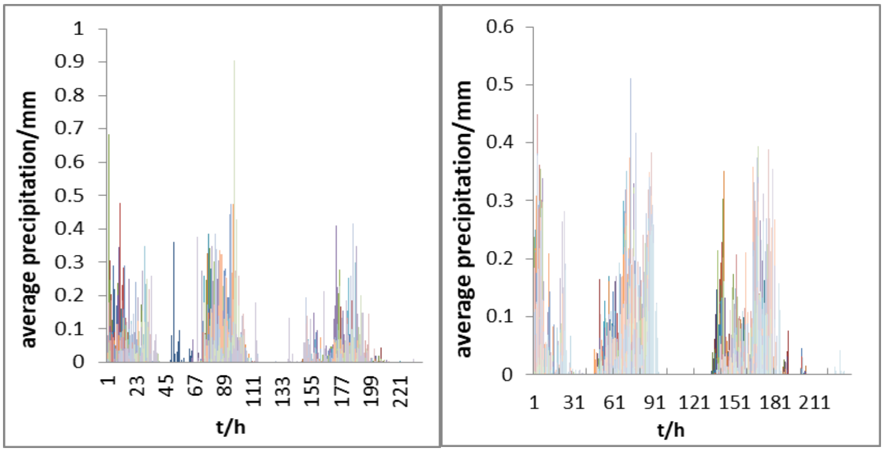

(a) (b)

Figure 5. Precipitation pattern comparison of two precipitation products(2008), (a) is the average precipitation of rain gauges, (b) is the average precipitation of PERSIANN-CCS QPEs.

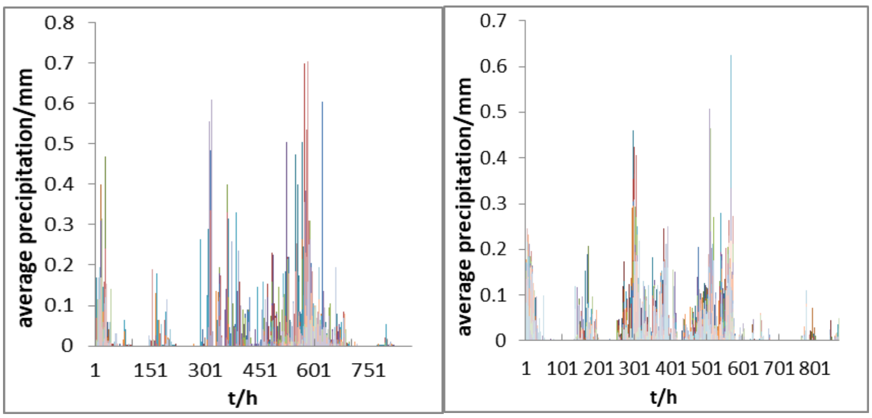

(a) (b)

Figure 6. Precipitation pattern comparison of two precipitation products(2009), (a) is the average precipitation of rain gauges, (b) is the average precipitation of PERSIANN-CCS QPEs.

Hydrol. Earth Syst. Sci. Discuss., https://doi.org/10.5194/hess-2018-438
Manuscript under review for journal Hydrol. Earth Syst. Sci.
Discussion started: 5 September 2018

Hydrology and Earth System Sciences
Open Access
Discussions

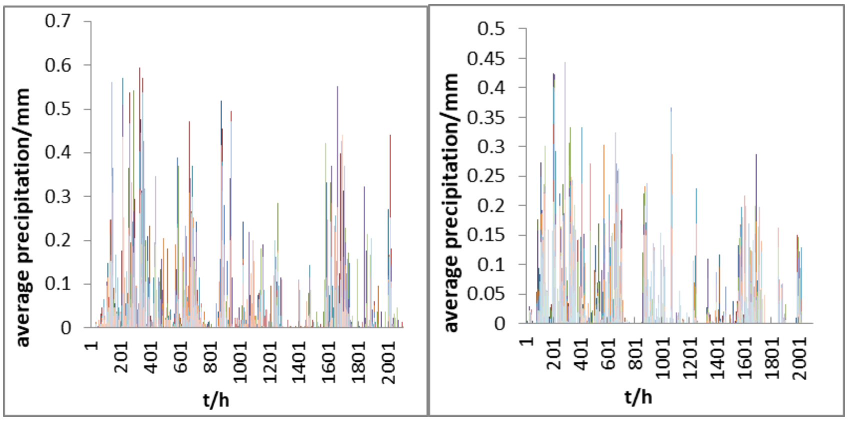

(a) (b)

Figure 7. Precipitation pattern comparison of two precipitation products(2011), (a) is the average precipitation of rain gauges, (b) is the average precipitation of PERSIANN-CCS QPEs.

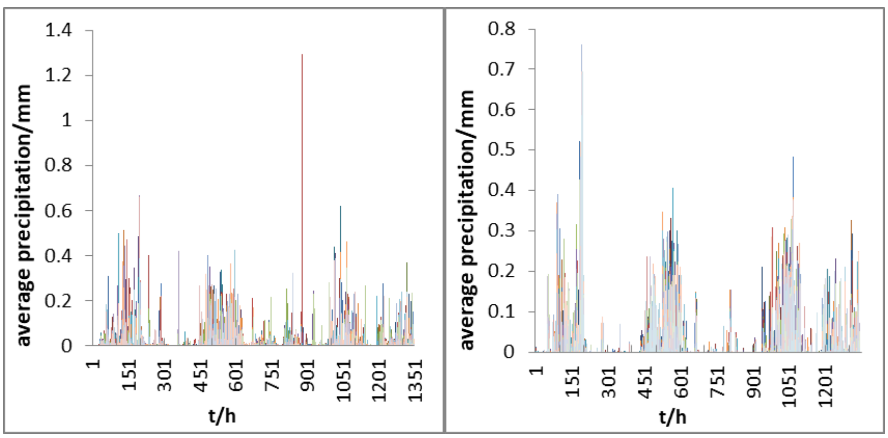

(a) (b)

Figure 8. Precipitation pattern comparison of two precipitation products(2012), (a) is the average precipitation of rain gauges, (b) is the average precipitation of PERSIANN-CCS QPEs.

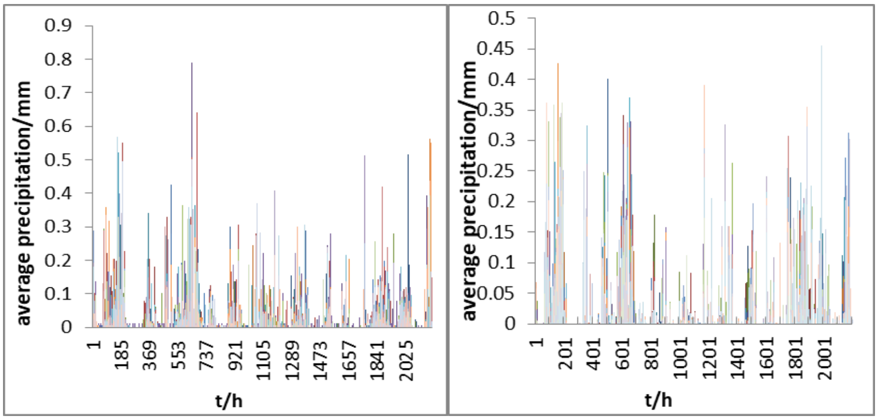

(a) (b)

Figure 9. Precipitation pattern comparison of two precipitation products(2013), (a) is the average precipitation of rain gauges, (b) is the average precipitation of PERSIANN-CCS QPEs.

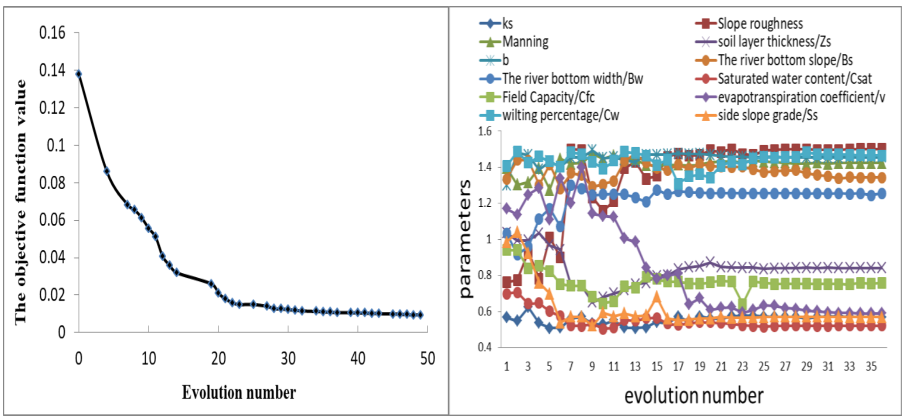

(a) The objective function evolution result (b) The parameters evolution result

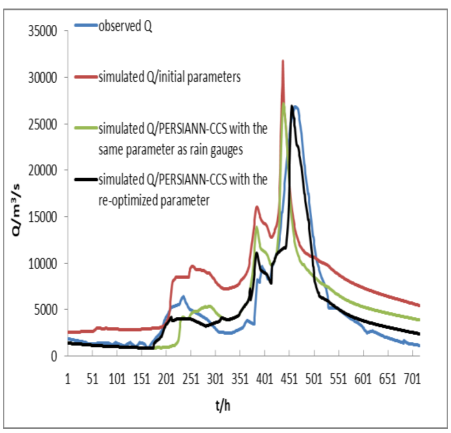

Hydrol. Earth Syst. Sci. Discuss., https://doi.org/10.5194/hess-2018-438
Manuscript under review for journal Hydrol. Earth Syst. Sci.
Discussion started: 5 September 2018

(c) The simulated flood process by using the optimized model parameters

Figure 10. Parameter optimization results with the improved PSO algorithm

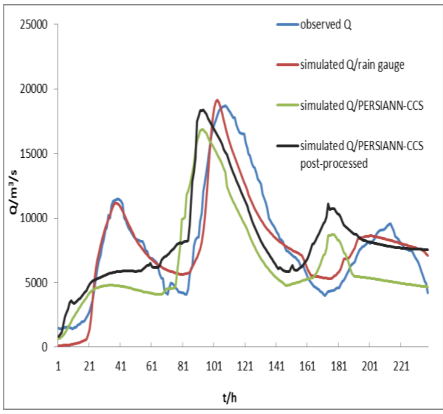

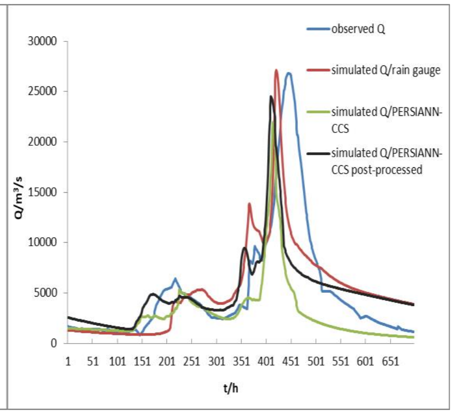

(a)flood event 200806090200 (b) flood event 200906090800

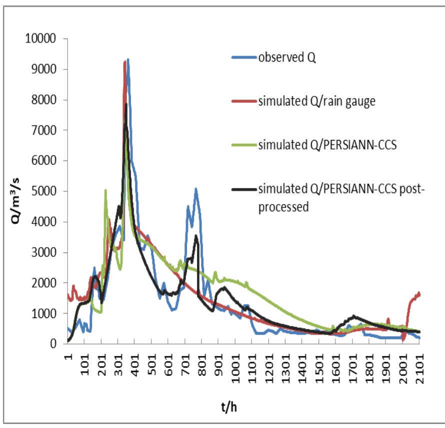

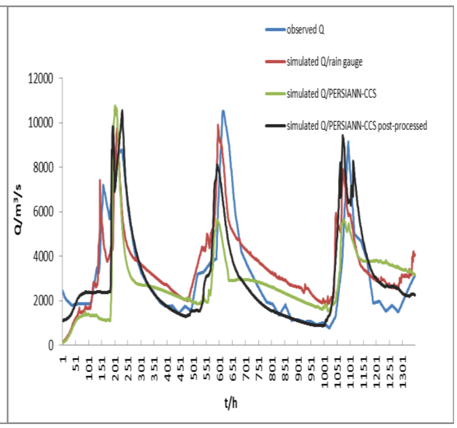

(c) flood event 201106010900 (d) flood event 201206022000

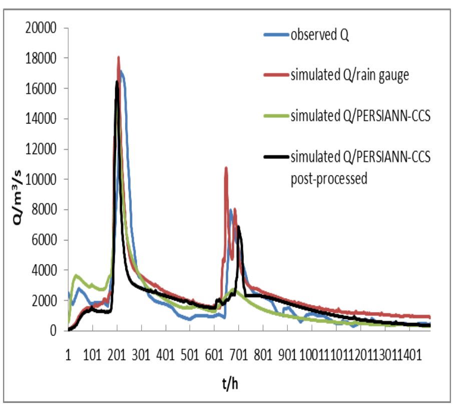

Hydrol. Earth Syst. Sci. Discuss., https://doi.org/10.5194/hess-2018-438
Manuscript under review for journal Hydrol. Earth Syst. Sci.
Discussion started: 5 September 2018

(e) flood event 201306011400

Figure 11. The flood simulation results of the coupling model with two precipitation products

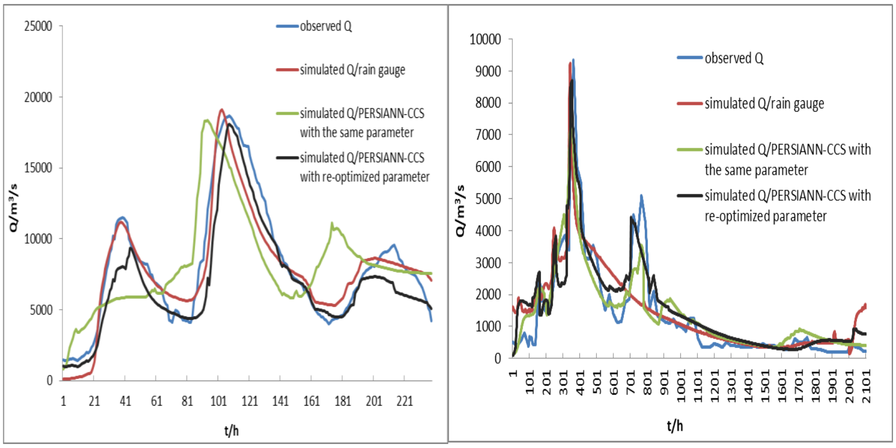

(a)flood event 200806090200 (b) flood event 201106010900

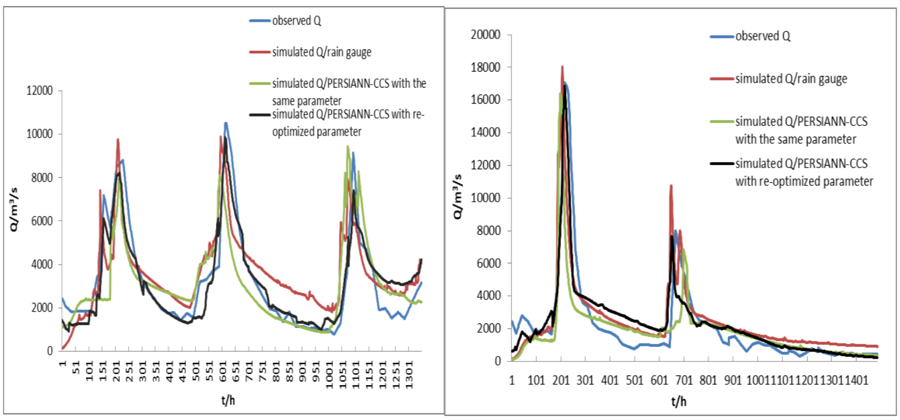

(c) flood event 201206022000 (d) flood event 201306011400

Figure 12. Coupled flood simulation results with the same parameter as the rain gauge precipitation and re-optimized parameter with the post-processed PERSIANN-CCS QPEs

Hydrol. Earth Syst. Sci. Discuss., https://doi.org/10.5194/hess-2018-438
Manuscript under review for journal Hydrol. Earth Syst. Sci.
Discussion started: 5 September 2018

Hydrology and Earth System Sciences
Discussions

Tables

Table 1. Precipitation pattern comparison of two precipitation products

flood	type	average precipitation(mm)	relative bias %
200806090200	rain gauge	0.37	
	PERSIANN-CCS QPEs	0.31	-16
200906090800	rain gauge	0.24	
	PERSIANN-CCS QPEs	0.18	-25
201106010900	rain gauge	0.22	
	PERSIANN-CCS QPEs	0.19	-14
201206022000	rain gauge	0.38	
	PERSIANN-CCS QPEs	0.30	-21
201306011400	rain gauge	0.22	
	PERSIANN-CCS QPEs	0.17	-23
average value	rain gauge	0.29	
	PERSIANN-CCS QPEs	0.23	-20

Table 2. The parameters of the coupling model

Parameters types	Name	Variable name	Physical property	Sensitivity	Adjustability
Evapotranspiration	Potential evaporation	Ep	Meteorology	insensitive	adjustable
	Evaporation coefficient	λ	Vegetation type	sensitive	adjustable
	Wilting percentage	Cwl	Vegetation type	insensitive	adjustable
The epikarst zone	Thickness	h	Soil type& Karst rock property	sensitive	unadjustable
	Saturated water content	θsat	Soil type	highly sensitive	adjustable
	Saturation permeability coefficient	θs	Soil type	highly sensitive	adjustable
	Wide crack volume ratio	V	Karst rock property	highly sensitive	adjustable
	Field capacity	θfc	Soil type	sensitive	adjustable
Rainfall-runoff	Soil layer thickness	z	Soil type	sensitive	adjustable
	Saturated hydraulic conductivity	Ks	Soil type	highly sensitive	adjustable
	Soil coefficient	b	Soil type	sensitive	adjustable
	Flow direction	Fd	Landform	highly sensitive	unadjustable

	Slope	S0	Landform	highly sensitive	unadjustable
	Bottom slope	Sp	Landform	sensitive	adjustable
	Bottom width	Sw	Landform	sensitive	adjustable
	Slope roughness	n	Landform &Vegetation type	sensitive	adjustable
	Channel roughness	n1	Landform &Vegetation type	sensitive	adjustable
The underground river	Depletion coefficient	ω	Landform &Soil type	sensitive	adjustable
	Muskingum routing method / The slope of the water storage content and flow curve	K	Landform	highly sensitive	adjustable
	Muskingum routing method/the proportion of the flow	χ	Landform	highly sensitive	adjustable

Table 3. Evaluation indices of simulated flood events with the post-processed PERSIANN-CCS QPEs

flood	type	Nash-Sutcliffe coefficient/C	Correlation coefficient/R	Process relative error/P%	Peak flow relative error/E%	The coefficient of water balance/W	Peak flow time error/T(h)
200806090000	rain gauge	0.8	0.91	15	3	0.89	-6
	PERSIANN-CCS QPEs	0.6	0.65	26	36	0.83	-69
	the post-processed PERSIANN-CCS QPEs	0.63	0.73	21	6	0.92	-60
200906090800	rain gauge	0.95	0.92	17	4	0.9	-12
	PERSIANN-CCS QPEs	0.67	0.61	28	34	0.79	-36
	the post-processed PERSIANN-CCS QPEs	0.75	0.64	22	14	0.85	-30
2011060	rain gauge	0.8	0.84	16	3	1.02	-7

10900	PERSIANN-CCS QPEs	0.65	0.83	25	21	0.89	-17
	the post-processed PERSIANN-CCS QPEs	0.75	0.85	21	12	0.92	-12
2012060 2200	rain gauge	0.82	0.79	20	5	0.8	-6
	PERSIANN-CCS QPEs	0.69	0.54	31	17	0.75	-21
	the post-processed PERSIANN-CCS QPEs	0.71	0.74	23	12	0.78	-15
2013060 11400	rain gauge	0.95	0.82	20	6	0.92	-4
	PERSIANN-CCS QPEs	0.7	0.84	28	10	0.79	-15
	the post-processed PERSIANN-CCS QPEs	0.82	0.89	24	7	0.85	-10
average value	rain gauge	0.86	0.86	18	4	0.91	-7
	PERSIANN-CCS QPEs	0.66	0.69	28	24	0.81	-32
	the post-processed PERSIANN-CCS QPEs	0.73	0.77	22	10	0.86	-25

874 Table 4. Evaluation indices of simulated flood events with different model parameters

flood	Parameter type	Nash-Sutcliffe coefficient/C	Correlation coefficient/R	Process relative error/P%	Peak flow relative error/E%	The coefficient of water balance/W	Peak flow time error/T(h)
2008060	rain gauge	0.8	0.91	15	3	0.89	-6

Hydrol. Earth Syst. Sci. Discuss., https://doi.org/10.5194/hess-2018-438
Manuscript under review for journal Hydrol. Earth Syst. Sci.
Discussion started: 5 September 2018

Hydrology and Earth System Sciences
Discussions

90000	Coupling model/the same model parameters as rain gauges	0.63	0.73	21	6	0.92	-60
	Coupling model/re-optimized model parameters	0.76	0.83	18	5	0.93	-4
2009060 90800	rain gauge	0.95	0.92	17	4	0.9	-12
	Coupling model/the same model parameters as rain gauges	0.75	0.64	22	14	0.85	-30
	Coupling model/re-optimized model parameters	0.82	0.78	19	7	0.87	-5
2011060 10900	rain gauge	0.8	0.84	16	3	1.02	-7
	Coupling model/the same model parameters as rain gauges	0.75	0.85	21	12	0.92	-12
	Coupling model/re-optimized model parameters	0.78	0.87	19	6	0.94	-10
2012060 2200	rain gauge	0.82	0.79	20	5	0.8	-6
	Coupling model/the same model parameters as rain gauges	0.71	0.74	23	12	0.78	-15
	Coupling model/re-optimized model parameters	0.78	0.76	21	8	0.79	-10
2013060	rain gauge	0.95	0.82	20	6	0.92	-4

11400	Coupling model/the same model parameters as rain gauges	0.82	0.89	24	7	0.85	-10
	Coupling model/re-optimized model parameters	0.86	0.91	22	6	0.87	-8
average value	rain gauge	0.86	0.86	18	4	0.91	-7
	Coupling model/the same model parameters as rain gauges	0.73	0.77	22	10	0.86	-25
	Coupling model/re-optimized model parameters	0.8	0.83	20	6	0.88	-7

References

Abbott, M. B., Bathurst, J. C., Cunge, J. A., O'Connell, P. E.,and Rasmussen, J.: An Introduction to the European HydrologicSystem-System Hydrologue Europeen, 'SHE', a: History and Philosophy of a Physically-based, Distributed Modelling System,J. Hydrol., 87, 45–59, 1986a.

Abbott, M. B.,Bathurst, J. C.,Cunge, J. A.,O'Connell, P. E., and Rasmussen, J.: An Introduction to the European Hydrologic System-System Hydrologue Europeen, 'SHE', b: Structure of a Physically based, distributed modeling System, J. Hydrol., 87,61–77, 1986b.

Ambroise, B., Beven, K., and Freer, J.: Toward a generalization of the TOPMODEL concepts: Topographic indices of hydrologic similarity, Water Resour. Res., 32,2135–2145, 1996.

Ashouri, H., Hsu, K.L., Soroosh,S., Braithwaite, D. K., Knapp, K. R., and Cecil, L. D.: PERSIANN-CDR: Daily Precipitation Climate Data Record from Multisatellite Observations for Hydrological and Climate Studies. Bulletin of the American Meteorological Society, 96(1):197-210, 2014.

Atkinson, T.C.: Diffuse flow and conduit flow in limestone terrain in the Mendip Hills, Somerset (Great Britain). Journal of Hydrology, 35(1-2):93-110, 1977.

Bartsotas, N., Nikolopoulos, E., Anagnostou, E., and Kallos, G.: Improving satellite quantitative precipitation estimates through the use of high-resolution numerical weather predictions: Similarities and contrasts between the Alps and Blue Nile region// EGU General Assembly Conference. EGU General Assembly Conference Abstracts, 2017.

Birk,S., Geyer, T., Liedl, R., and Sauter, M.: Process-based interpretation of tracer tests in carbonate aquifers. Ground Water, 43(3): 381-388, 2005.

Chen, Y.B, Li, J., Wang, H., Qin, J., and Dong, L.: Large-watershed flood forecasting with high-resolution distributed hydrological model, Hydrol. Earth Syst. Sci., 21, 735–749, doi:10.5194/hess-21-735-2017, 2017.

Chen, Y.B., Li, J., and Xu, H.J.: Improving flood forecasting capability of physically based distributed hydrological models by parameter optimization, Hydrol. Earth Syst. Sci., 20, 375–392, doi:10.5194/hess-20-375-2016, 2016.

Chen, Y.B.: Liuxihe Model, China Science and Technology Press, Peking, China, September 2009.

Davis W.M.: Relation of geography to geology. Geological Society of America Bulletin, 23,1912.

Delrieu,G., Bonnifait, L., Kirstetter, P. E., and Boudevillain, B.: Dependence of radar quantitative precipitation estimation error on the rain intensity in the Cévennes region, France. Hydrological Sciences Journal, 59(7):1308-1319,2014.

Doummar, J., Margane, A., Sauter, M., and Geyer, T.: Assessment of transport parameters in a karst system under various flow periods through extensive analysis of artificial tracer tests// EGU General Assembly Conference. EGU General Assembly Conference Abstracts, 2012.

Duan, J.,and Miller,N.L.: A generalized power function for the subsurface transmissivity profile in TOPMODEL. Water Resources Research, 33(11):2559–2562, 1997.

Falorni, G., Teles, V., Vivoni, E. R., Bras, R. L., and Amaratunga, K. S.: Analysis and characterization of the vertical accuracy of digital elevation models from the Shuttle RadarTopography Mission, J. Geophys. Res.-Earth, 110, F02005, doi:10.1029/2003JF000113, 2005.

Faure, D., Gaussiat, N., Tabary, P., and Urban, B.: Real time integration of foreign radar quantitative precipitation estimations (QPEs) in the French national QPE mosaic// Conference on Radar Meteorology, AMS,21-21, 2015.

Ford, D., and Williams P.W.: Karst Geomorphology and Hydrology. Geographical Journal, 157(1):87,1991.

Freeze, R. A. and Harlan, R. L.: Blueprint for a physically-based,digitally simulated, hydrologic response model, J. Hydrology., 9,237–258, 1969.

Goldscheider, N., and Drew, D.: Methods in Karst Hydrogeology: IAH:International Contributions to Hydrogeology, 26. CRC Press, 2007.

Goudenhoofdt E, Delobbe L.: Evaluation of radar-gauge merging methods for quantitative precipitation estimates. Hydrology & Earth System Sciences, 13(2):195-203.,2009.

Hartmann, A., Barberá, J. A., Lange, J., Andreo, B., and Weiler, M.: Progress in the hydrologic simulation of time variant recharge areas of karst systems – Exemplified at a karst spring in Southern Spain. Advances in Water Resources, 54(2):149-160, 2013.

Hirpa, F. A., Gebremichael, M., and Hopson, T.: Evaluation of high-resolution satellite precipitation products over very complex terrain in ethiopia. J.appl.meteor.climatol, 49(5), 1044-1051.,2010.

Hsu, K. L., Gupta, H. V., Gao, X.G, and Soroosh,S.: Estimation of physical variables from multichannel remotely sensed imagery using a neural network: Application to rainfall estimation. Water Resources Research, 35(5):1605-1618,1999.

Hydrol. Earth Syst. Sci. Discuss., https://doi.org/10.5194/hess-2018-438
Manuscript under review for journal Hydrol. Earth Syst. Sci.
Discussion started: 5 September 2018

Hsu, K.L, Yang,H., and Soroosh,S.: Rainfall Estimation Using a Cloud Patch Classification Map// Measuring Precipitation From Space. Springer Netherlands,329-342, 2007.

Hussain, Y., Satgé, F., Hussain, M. B., Martinez-Carvajal, H., Bonnet, M. P., and Cárdenas-Soto, M.: Performance of CMORPH, TMPA, and PERSIANN rainfall datasets over plain, mountainous, and glacial regions of Pakistan. Theoretical & Applied Climatology, 131(3-4), 1119-1132,2018.

Hu, Q.F., Yang,D.W.,Wang,Y.T.,Yang,H.B.,and Liu,Y.: Characteristics and sources of errors in daily ＴＲMM precipitation product over Ganjiang River basin in China．ADVANCES IN WATER SCIENCE,24(6)：794-800,2013.

Kovacs,A., and Perrochet,P.: Hydrograph Analysis for Parameter Estimation of Connected and Karst Systems// Engineers Australia, 2011.

Li, J., Chen, Y.B., Wang, H.Y., Qin, J.M., Li, J., and Chiao, S.: Extending flood forecasting lead time in a large watershed by coupling WRF QPF with a distributed hydrological model. Hydrology & Earth System Sciences Discussions, 21:1-45,2017.

Li,B.G.,and Tao,S.: Several Problems and Their Solutions in Surface Runoff Modeling. Bulletin of Soil and W ter Conservation, 20(3):47-49,2000.

Li,G.F.: Karst Hydrogeologic Characteristics and Water Resources in Guangxi,China, Carsologica Sinica,3:253-258,1996.

Li,X.M., and Ren,B.: The calculation method of non-closure small watershed of the mine water runoff in ungauged basins. Mineral Engineering Research, 2009.

Liu,H.M.Deng,H.P.,Sun,S.F.,and Xiao,Y.: .Numerically Test of Influence of Incorporation of TOPMODEL into Land Surface Model SSiB on Hydrological Simulation at Basin Scale.PLATEAU METEOROLOGY, 32(3):829-838,2013.

Liu, X.Y.,Yang, T., Hsu ,K.L., Liu, C., and Soroosh,S.: Evaluating the streamflow simulation capability of PERSIANN-CDR daily rainfall products in two river basins on the Tibetan Plateau. Hydrology & Earth System Sciences Discussions, 21(1):1-31, 2017.

Loveland, T. R., Merchant, J. W., Ohlen, D. O., and Brown, J. F.: Development of a Land Cover Characteristics Data Base for the Conterminous U.S., Photogram, Photogramm. Eng. Rem. S., 57, 1453–1463, 1991.

Loveland, T. R., Reed, B. C., Brown, J. F., Ohlen, D. O., Zhu, J., Yang, L., and Merchant, J. W.: Development of a Global Land Cover Characteristics Database and IGBP DISCover from 1-km AVHRR Data, Int. J. Remote Sens., 21, 1303–1330, 2000.

Liang,H.: Prelim in Ary Study on the Characteristics of Flood Discharge and Low Flow in Fluenced by the Scale of Karst Dranin Age Basin- Exampled by the River s in Guizhou Province,China, Carsologica Sinica. 2:121-129, 1997.

Moradkhani, and Meskele, T.T.: Satellite Rainfall Applications for Surface Hydrology. Springer Netherlands, 2010.

Neitsch,S.L.,J.G.Arnold,J.R.Kiniry and J.R.Williams.: Soi1 and Water Assessment Tool Theoretical Documentation Version,2000.

Quinlan, J.F and Ewers, R.O.: Ground water flow in limestone terranes -strategy, rationale and procedure for reliable, efficient monitoring of ground water in karst areas. Mendeley, 8:167-173, 1985.

Quinlan, J. F., Davies, G. J., Jones, S. W., and Huntoon, P. W.: The applicability of numerical models to adequately characterize ground-water flow in karstic and other triple-porosity aquifers. 1288:114-

Hydrol. Earth Syst. Sci. Discuss., https://doi.org/10.5194/hess-2018-438
Manuscript under review for journal Hydrol. Earth Syst. Sci.
Discussion started: 5 September 2018

Hydrology and Earth System Sciences
Discussions

133, 2011.

Rafieei,N.A., Norouzi,, A., Kim, B., and Seo, D.: J Fusion of multiple radar-based quantitative precipitation estimates (QPE) for high-resolution flash flood forecasting in large urban areas// AGU Fall Meeting. AGU Fall Meeting Abstracts, 2014.

Ren,Q.W.: Water Quantity Evaluation Methodology Based on Modified SWAT Hydrological Modeling in Southwest Karst Area. China University of Geoscience, Wuhan ,China, 2006.

Romill, T. G. and Gebremichael, M.: Evaluation of satellite rainfall estimates over Ethiopian river basins. Hydrol. Earth Syst. Sci., 15, 1505–1514, 2011, doi:10.5194/hess-15-1505-2011.

Saxton, K.E, Rawls, W. J, Romberger, J .S, and Papendick, R. I.: Estimating generalized soil water characteristics from texture. Soil Science Society of America Journal, 50: 1031- 1036,1986.

Servat, E .,and Sakho,M.: Modelling and management of sustainable basin-scale water resource systems : proceedings of an international symposium held at Boulder, Proceedings of IAHS Symposium 6, IAHS Publication No.231,1995.

Sharma, A. and Tiwari, K. N.: A comparative appraisal of hydrological behavior of SRTM DEM at catchment level, J. Hydrol., 519, 1394–1404, 2014.

Shuster, E .T, and White,W.B.: Seasonal fluctuations in the chemistry of lime-stone springs: A possible means for characterizing carbonate aquifers. Journal of Hydrology, 14(2):93-128,1971.

Soroosh,S., Hsu ,K.L.,Gao,,X.G.,Hoshin,V.G.,Bisher,I.,and Braithwaite, D.: Evaluation of PERSIANN System Satellite-Based Estimates of Tropical Rainfall. Bulletin of the American Meteorological Society,81,2035-2046,2000.

Stenz, R.D.: Improving satellite quantitative precipitation estimates by incorporating deep convective cloud optical depth. Dissertations & Theses - Gradworks, 2014.

Strahler, A. N.: Quantitative analysis of watershed Geomorphology,Transactions of the American Geophysical Union, 35, 913–920,1957.

Tan ,M.L., and Santo,H.: Comparison of GPM IMERG, TMPA 3B42 and PERSIANN-CDR satellite precipitation products over Malaysia. Atmospheric Research, , 202, 2018.

Wardhana A, Pawitan H, and Dasanto B D.: Application of hourly radar-gauge merging method for quantitative precipitation estimates//012033,2017.

Williams,P.W.: Geomorohic inheritance and the development of tower karst Earth surface Progresses and landform.12,453-465,1987.

Yang,H., Hsu, K. L., Soroosh,S., and Gao, X.G.: Precipitation Estimation from Remotely Sensed Imagery Using an Artificial Neural Network Cloud Classification System. Journal of Applied Meteorology, 36(9):1176-1190,2004.

Yang,H.,Gochis, D., Cheng, J. T., Hsu, K. L., and Soroosh,S.: Evaluation of PERSIANN-CCS Rainfall Measurement Using the NAME Event Rain Gauge Network. Journal of Hydrometeorology, 8(3):469, 2007.

Zhang,C.,Jiang,Y.J.,Lian,Y.Q.,Yuan,D.X.,Pei,J.G.,and Jiang,G.H.: Rainfall-runoff simulation of a typical karst fengcong depression system using SWMM model-A case study of the Yaji experimental site in Guilin.Hydrogeology and Engineering Geology,34(3):10-14, 2007.